International Journal of Naval Architecture and Ocean Engineering 12 (2020) 657–666

Contents lists available at ScienceDirect

International Journal of Naval Architecture and Ocean Engineering

journal homepage: http://www.journals.elsevier.com/international-journal-of-naval-architecture-and-ocean-engineering/

An advanced technique to predict time-dependent corrosion damage of onshore, offshore, nearshore and ship structures: Part I = generalisation

Do Kyun Kim [a, b], Eileen Wee Chin Wong [c], Nak-Kyun Cho [d, *]

[a] Marine Offshore and Subsea Technology Group, Newcastle University, NE1 7RU, Newcastle upon Tyne, UK
[b] Graduate Institute of Ferrous Technology, POSTECH, 37673, Pohang, South Korea
[c] Ocean & Ship Technology (OST) Research Group, Universiti Teknologi PETRONAS, 32610, Seri Iskandar, Perak, Malaysia
[d] Department of Manufacturing Systems and Design Engineering, SeoulTech, 01811, Seoul, South Korea

A R T I C L E I N F O

Article history:
Received 17 March 2020
Received in revised form
11 June 2020
Accepted 25 June 2020
Available online 24 August 2020

Keywords:
Corrosion modelling
Time-dependent
Non-linear corrosion
Aging
Engineering

A B S T R A C T

A reliable and cost-effective technique for the development of corrosion damage model is introduced to predict nonlinear time-dependent corrosion wastage of steel structures. A detailed explanation on how to propose a generalised mathematical formulation of the corrosion model is investigated in this paper (Part I), and verification and application of the developed method are covered in the following paper (Part II) by adopting corrosion data of a ship's ballast tank structure. In this study, probabilistic approaches including statistical analysis were applied to select the best fit probability density function (PDF) for the measured corrosion data. The sub-parameters of selected PDF, e.g., the largest extreme value distribution consisting of scale, and shape parameters, can be formulated as a function of time using curve fitting method. The proposed technique to formulate the refined time-dependent corrosion wastage model (TDCWM) will be useful for engineers as it provides an easy and accurate prediction of the 1) starting time of corrosion, 2) remaining life of the structure, and 3) nonlinear corrosion damage amount over time. In addition, the obtained outcome can be utilised for the development of simplified engineering software shown in Appendix B.

1. Introduction

Corrosion is one of the most critical factors causing degradation of aging infrastructures such as onshore, offshore, and subsea structures. It is a major threat to the structural integrity of aging structures. It poses challenges to the operation of metal structure (especially for offshore, subsea, and ship structures) as it degrades the structure and reduces the safety level of the structure. Corrosion leads to loss of metal cross-section and results in a decrease of structural strength and capacity. It is well recognised that corrosion damage becomes more severe as the structure ages. When approaching the end of the operating life (i.e., design life), the possibility of the structure to fail without any warning significantly increases. To ensure safe operation of structure, assessment of the defects on the structure should be performed.

Fig. 1(a) shows corroded platform legs in the Gulf of Mexico that were at risk of losing structural integrity. If no proper treatment is taken on the corroded structure, corrosion will lead to leakage, equipment failure, loss of containment of process fluids, and environmental pollution. In the worst-case scenario, it may cause serious accidents and eventually loss of lives. Corrosion can also occur in any subsystems within oil and gas production system including pipelines.

The EU's eMARS database, which records all accidents reported to the European Commission, indicates that 20% of the 137 major refinery accidents occur mainly due to corrosion failure. External and internal corrosions, material failure, and third-party interference are the leading causes of pipe-related incidents, responsible for over 75% of the total incidents between 2002 and 2013 (Lam, 2015). Fig. 1(b) shows Maltese tanker Erika that suffered from

* Corresponding author.
E-mail address: nkcho@seoultech.ac.uk (N.-K. Cho).
Peer review under responsibility of Society of Naval Architects of Korea.

https://doi.org/10.1016/j.ijnaoe.2020.06.007

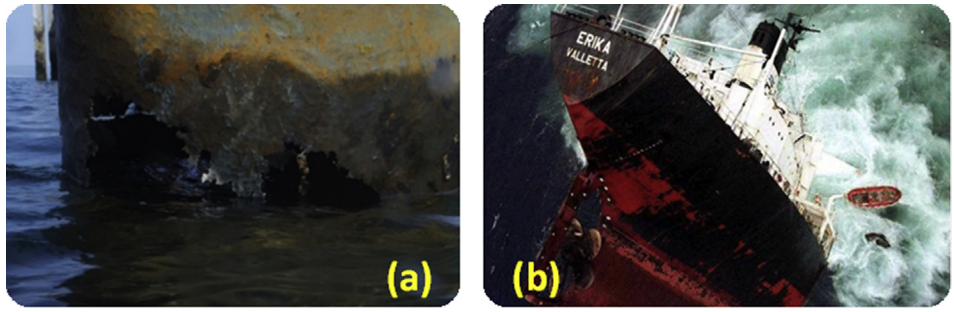

Fig. 1. Examples of corroded structures; (a) Offshore jecket platform (Commercial and Specialised Diving LTD, 2018); (b) Oil tanker Erika (Energy Global News, 2020).

corrosion and broke into two parts due to hogging bending moment at the coast of Brittany at France Sea causing tremendous oil spills. Hence, structural reliability analysis of the corrosion-damaged ship and other offshore structures is essential.

To assess corrosion damage on the structure, its corrosion rate should be estimated in advanced with care (Chernov and Ponomarenko, 1991). With regards to this, reliable data processing technique shall be required. The importance of data processing techniques including artificial neural network (ANN) (Wong and Kim, 2018), regression analysis including probabilistic techniques (Kim et al., 2019a; b), fuzzy concept (Abdussamie et al., 2018) and many others have also been highlighted.

Numerous studies have been performed to evaluate corrosion damage of metal structures and develop corrosion models for predicting corrosion rate. Corrosion models can be categorised into two groups: physical and empirical models. The physical model is derived based on the physical corrosion process, whereas the empirical model is developed using historical data of the corrosion wastage measurement of existing structures (Paik and Melchers, 2008).

Evans (1960) and Tomashov (1966) developed a physical corrosion model based on the proposition that the corrosion process is controlled by ion transportation through corrosion product or rust layer. Chernov (1990) proposed a model for predicting corrosion of steels in seawater by relating the changes in steel corrosion with time to the aggressiveness of seawater. Chernov and Ponomarenko (1991) adopted a similar concept, but with the addition of semi-empirical correction factor, considering the effects of seawater temperature, velocity, and salinity effects. Melchers (2003a) identified the non-linearity relationship of corrosion with time. He developed a corrosion model that represents the corrosion progress over time by including the effects of environmental and material factors in immersion corrosion. Melchers (2003b) also developed a mathematical model that allows for a non-uniform build-up of corrosion product and the consequent slowing of the corrosion process. A detailed review of physical corrosion modelling in marine environments is summarised by (Paik and Melchers, 2008; Melchers, 2008).

Different empirical corrosion models were developed in the past. Paik and Thayamballi (2007) developed several time-dependent corrosion wastage models for different ship structures. Based on their investigation, corrosion measurement data indicated scatterings of corrosion damage at any exposure time and that corrosion varies with time. They performed statistical analysis of the collected corrosion data and proposed a mathematical function named the time-dependent corrosion wastage model. Melchers (2003c) also proposed a probabilistic model for at sea immersion corrosion of mild and low alloy steels based on fundamental physiochemical corrosion mechanics. Paik and Kim (2012) established an advanced method of developing time-dependent corrosion wastage model by applying probability density as a function of the age of the structure. Several researchers have proposed different empirical ship corrosion wastage models as well (Paik et al., 1998, 2003a; b; 2004).

Besides ship structure, empirical models of corrosion damage for other structures were also investigated. Mohd Hairil and Paik (2013) analysed the statistical data of oil well tube corrosion and identified 2-parameter Weibull function to be suitable for describing corrosion progress of oil well tubes. Akpa Jackson (2013) proposed empirical model equations to predict the corrosion rates of the two stainless steel grades in marine oil environment using the principle of dimensional analysis of Buckingham π theorem. Mohd Hairil and Paik (2013) and Mohd Hairil et al. (2014a, 2014b) proposed a time-dependent pit depth corrosion model for well tubes and subsea gas pipelines, respectively, using 3-parameter Weibull distribution function. In addition, the effects of corrosion on the structural safety assessment of ships and offshore structures have also been studied by several researchers (Qin and Cui, 2003; Wang et al., 2008; Kim et al., 2012a, b, c; 2014a; b; 2015; Wood et al., 2013; Gucuyen and Erdem, 2014; Rahbar-Ranji et al., 2015; Zhang et al., 2016; Meo and Oterkus, 2017; Cheng and Chen, 2017; Kim et al., 2017; Ringsberg et al., 2018; Cui et al., 2019).

Recently, studies on the development of time-dependent corrosion wastage model have further progressed by conducting corrosion test considering room and low temperatures for material grade A, AH32 and DH 32 (Rajput et al., 2019). The effect of mechanical stress (Yang et al., 2016) and the estimation technique for corrosion rate (Ivošević et al., 2019) have also investigated. Moreover, the application studies have also conducted such as wave-induced hull girder bending stresses and section modulus (Ivanov and Chen, 2017), reliability assessment of offshore fixed platform (Bai et al., 2016), hull girder strength (Georgiadis and Samuelides, 2019).

In this study, a general time-dependent corrosion damage model and the developing procedure, which can provide simple and clear mathematical formulations, are proposed using probabilistic approach by utilising probability density function to determine non-linear corrosion growth over several years. This corrosion model can aid in determining the corrosion rate of the structure as well as predicting the remaining life of the structure for deciding the suitable time to repair and retrieve the corroded structure.

2. Limitation of existing techniques

In this section, the problem statements are discussed to state the apparent reason why advanced techniques and procedures are required to propose the generalised time-dependent corrosion model. In recent years, the low oil prices and weak demands have affected the oil and gas industry. The oil-and-gas downturn triggers the industry to cut down the expenditure for upstream business. Consequently, many companies strive to operate structures as close to their maximum capacity while ensuring the safety of the structure. The current practice uses deterministic approach and linear corrosion growth model to estimate corrosion depth. This approach gives conservative result and overestimates the corrosion depth causing early retrieval and decommissioning of structures, though the structure can still operate much longer. Thus, time-dependent non-linear corrosion model is required for more accurate estimation of the corrosion depth of the structure.

With regards to this, several types of time-dependent corrosion wastage model (TDCWM) and techniques were proposed and applied to ships and offshore structures such as linear TDCWM (Paik et al., 2003a, 2003b; 2004), and nonlinear TDCWM (Guedes Soares et al., 2005; Paik and Kim, 2012; Mohd Hairil and Paik, 2013; Mohd Hairil et al., 2014a, 2014b). In the case of the linear shape of TDCWM, it provides the amount of annual corrosion damage (mm/year) which means that time (year) and corrosion damage (mm) are linearly related. In the case of the nonlinear shape of TDCWM, this model can help to predict a more accurate amount of corrosion damage than the linear model.

However, the proposed method and obtained nonlinear corrosion models from the previous studies have a technical limitation in the direct calculation (or prediction) of the corrosion damage amount. The previous proposed corrosion models (Paik and Kim, 2012; Mohd Hairil and Paik, 2013; Mohd Hairil et al., 2014a, 2014b) predict the probability density of corrosion damage (mm) by time shown in Eq. A.1 in Appendix A rather than the direct prediction of corrosion damage (mm) by time. From the previous method, engineers should calculate corrosion damage amount again based on mean and standard deviation and further simplification process need to be conducted.

To simplify the abovementioned steps, a generalisation method for developing accurate nonlinear time-dependent corrosion wastage model is proposed based on advanced data processing technique in Part I. The proposed technique in this study is introduced in next section. The proposed technique is verified by ship's ballast tank corrosion data in Part II (Kim et al., 2020). Based on proposed technique, useful software has been developed and briefly introduced in Appendix B part in this study.

3. Procedure of proposed technique for the development of corrosion model

Corrosion is one of the age-related damages experienced by most ships and offshore structures. As the structure operating age increases, the corrosion depth along the structure increases while the thickness of the structure reduces. The distribution of the corrosion depth follows a specific probability distribution. The corrosion depth distribution over the years can be used to estimate the growth of corrosion depth. In the present section, a detailed procedure to propose the advanced time-dependent corrosion wastage model in the form of a mathematical formulation is presented.

3.1. Research questions

Previously, Paik and Thayamballi (2003) raised the following research questions.

- Where is corrosion likely to occur?
- When does it start?
- What is its extent?
- What are the likely corrosion rates as a function of time?

In the present study, the following research questions are prepared to frame the existing corrosion issues to be resolved by the present study.

- How does corrosion grow with time?
- Which probability distribution function is suitable to study the distribution of corrosion depth for each year?
- When does corrosion start?
- How can the remaining life of the structure be estimated from the time-dependent corrosion damage model?

3.2. Proposed solution

In this section, the procedure for the development of corrosion model is introduced in Fig. 2. Based on the proposed method, time-dependent corrosion wastage model for ship's ballast tank is developed in Part II (Kim et al., 2020). In this paper, few examples have been added in Steps 1 to 10 to provide better understanding to the readers, however, the example data is not related to each other.

3.2.1. Collection of corrosion data at various times (Step 1)

In the first stage, a collection of measured corrosion data is required. In general, corrosion data is measured by using the following methods:

- Pigging testing (Onshore/Offshore pipeline)
- Ultrasonic testing
- Radiographic testing
- Electromagnetic testing
- Permanent cathodic protection monitoring

3.2.2. Validation of data type and selection of the best interval (Step 2)

The collected corrosion data can then be validated based on data types such as general time data set or specific time data set. Samples of both corrosion data sets are presented in Fig. 3(a) and (b) which show the difference classified by corrosion interval.

In the case of specific time data set, it is unnecessary to find the best interval by time, which means that the collected specific time data set will directly be used as input data for the goodness of fit-test step. In the case of general time data set in Fig. 3(b), which can be obtained from real-time corrosion monitoring system or regularly scheduled corrosion inspections (frequent inspection case), additional tests need to be conducted to determine the best interval with respect to time.

3.2.3. Selection of best interval (Step 3)

For the selection of the best-fitted interval, the following methods are recommended in general (Kim et al., 2020). The reason that the following methods should be implemented is to find the relevant interval that will be used as a basic input to generate an individual histogram. The obtained histogram needs to be well-representing the input corrosion damage characteristics. Determination of the best interval was recently investigated by Joo et al. (2018). In addition, Statisticians widely studies how to select best intervals by adopting non-uniform interval concept while, simplified methods are suggested and adopted in this study.

- Minimum coefficient of variation (COV) and maximum mean value method
- R^2 method
- Sturges method
- Scott method

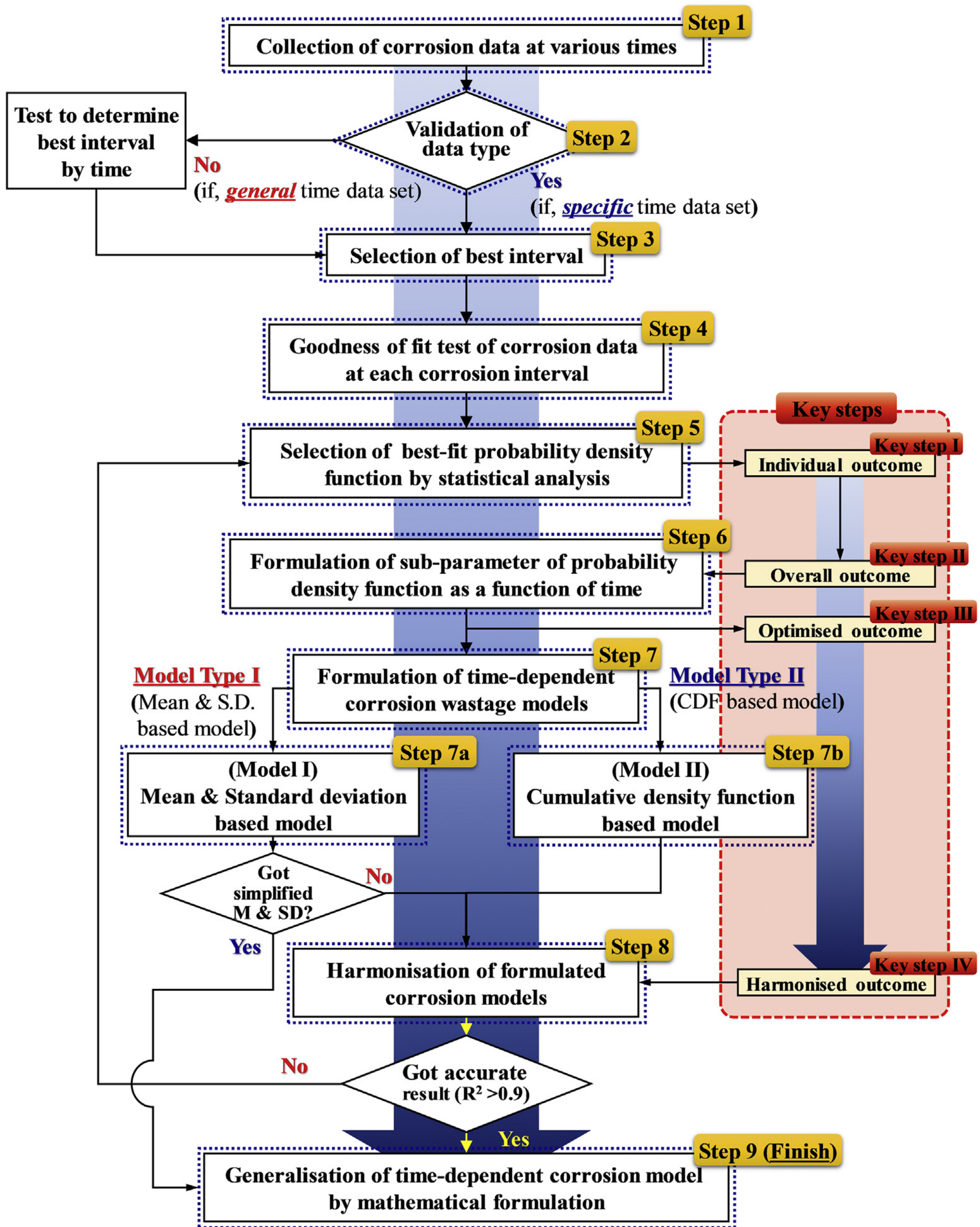

Fig. 2. Procedure of proposed method (Note: M = Mean, and SD = standard deviation).

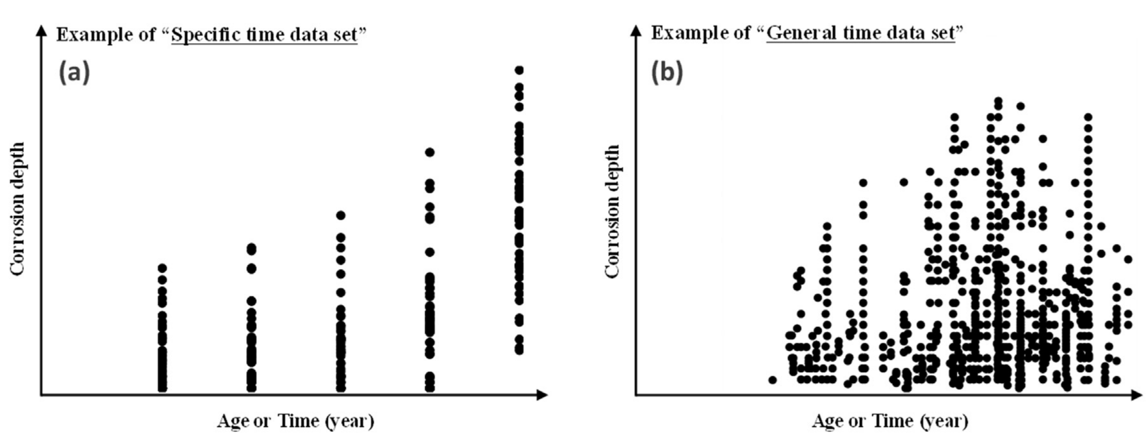

Fig. 3. Example of corrosion input data; (a) Specific time data set; (b) General time data set.

Table 1
Example of the selection of best-fit probability density function.

Ranking	Test methods					
	A-D test	C–S test	H-L test	K–S test	S–W test	Others
1	**LEV**	**LEV**	Weibull	**LEV**	Normal	⋮
2	Normal	Weibull	LEV	Normal	LEV	⋮
3	Weibull	Normal	Normal	Weibull	Weibull	⋮
⋮	⋮	⋮	⋮	⋮	⋮	⋮

Note: LEV = Largest Extreme Value.

- Freedman method
- Shikamazi and Shinomoto method.

Once the best interval is selected, corrosion data can then be shown as specific time data set as shown in Fig. 3(a).

3.2.4. Goodness of fit test of corrosion data at each corrosion interval (Step 4)

Once the best-interval is selected, which also means that the histogram is ready to be plotted based on collected specific corrosion time data set, the goodness of fit test is then conducted to find the best-fit probability density function (PDF). The following test methods are suggested in conducting the statistical analysis. Details of goodness of fit tests may be referred to Wikipedia (2018).

Types of goodness of fit test.

- Anderson–Darling (A-D) test
- Akaike information criterion
- Chi-squared (C–S) test
- Cramér–von Mises criterion
- Hosmer–Lemeshow (H-L) test
- Kolmogorov–Smirnov (K–S) test
- Kolmogorov–Smirnov (K–S) test
- Shapiro–Wilk (S–W) test
- Others

3.2.5. Selection of the best-fit probability density function by statistical analysis (Step 5)

The abovementioned goodness of fit tests can sort the test values from the existing PDF, which means that test values can be listed down in ascending order as shown in Table 1. The smallest value obtained by the goodness of fit test will be considered as the best-fit probability density function (PDF). Fig. 4 shows a typical example of the goodness of fit test by adopting the Anderson-Darling (A-D) test and all of them show the selected best fit PDF. Table 2 shows the detail of the A-D test results. For example, normal distribution gives the smallest A-D value of 0.16; hence, it is selected as the best fit PDF for data 1. Details may be referred to Key Step I and II.

Furthermore, the abovementioned various goodness of fit test methods can provide slightly different best-fit PDFs for each annual dataset. Regarding this, it is suggested that the best fit PDF can be achieved based on the most frequent best-fit PDF from the different test methods. For example, if one of the probability distributions is the most repeated PDF among all the test methods shown in Table 1, it is then considered as the best-fit distribution which best represents the behaviour of collected corrosion data with the highest accuracy. Table 1 shows the example of the selection of best-fit PDF using different test methods. In this example, the largest extreme value distribution, which is the most repeated, can be selected as the best-fit PDF.

- Individual outcome (Key step I)

As indicated in Fig. 2, there are four (4) key steps with nine (9) general steps to develop time-dependent corrosion wastage model. First, individual best probability density functions (herein, defined as individual outcome) can be determined. Once specific time data set is obtained as presented in Fig. 3(a), the best-fit PDF is then investigated for the selected or obtained specific time data set by adopting the goodness of fit test as explained in Step 5.

Table 2 shows a relevant example of the goodness of fit test results for five (5) different time data sets that have been used as inputs. For better understanding, individual outcomes are highlighted in bold print in Table 2. As highlighted, Data 1 to 5 have different best-fit PDFs such as Normal, Logistic, 3-Parameter Loglogistic, 3-Parameter Lognormal, and Largest Extreme Value distributions, respectively. All those selected individual best PDFs are based on the lowest value by the goodness of fit test. In some cases, the same PDF may be selected as the best-fit PDF. Hence, the selected five best-fit PDFs can be defined as “individual outcome” from the example in Table 2.

In conclusion, the important features of individual outcome are summarised such that, 1) it provides the individual best-fit probability density functions, 2) it reflects the corrosion behaviour in the best way, 3) the obtained individual outcome does not directly provide time-dependent corrosion model; which indicate that additional processing needs to be performed to obtain the simplified corrosion model. Fig. A1(a) shows an example of the individual outcome. As expected, individual outcome represents accurate individual corrosion behaviour from selected time data sets. However, it needs to be coalesced to propose the corrosion model via mathematical formulation.

- Overall outcome (Key step II)

In the previous Key step I, individual outcomes have been achieved. The overall outcome can be obtained based on the average value from individual outcomes as calculated in Table 2, which shows that the largest extreme value distribution has been selected based on 0.95 goodness of fit test value that gave the smallest average value among others.

Once the overall outcome is obtained, it can be applied to other corrosion data sets at different time. This means that once the best-fit PDF is selected, it will then be subjected to the all-time data set. This step may bring restrained accuracy to the result, however, it may also help to provide a possible formulation for the corrosion model. The accuracy of the outcome with different methods will be investigated in Part II discussion section (Kim et al., 2020). The example of overall outcome can be referred to Fig. A1(b). Once again, in the example, the largest extreme value distribution is selected in Table 2 but other types of distribution can also be selected for the different case. Further processing work needs to be conducted in Key step III and IV, which will be documented together in the following Steps 6 to 9.

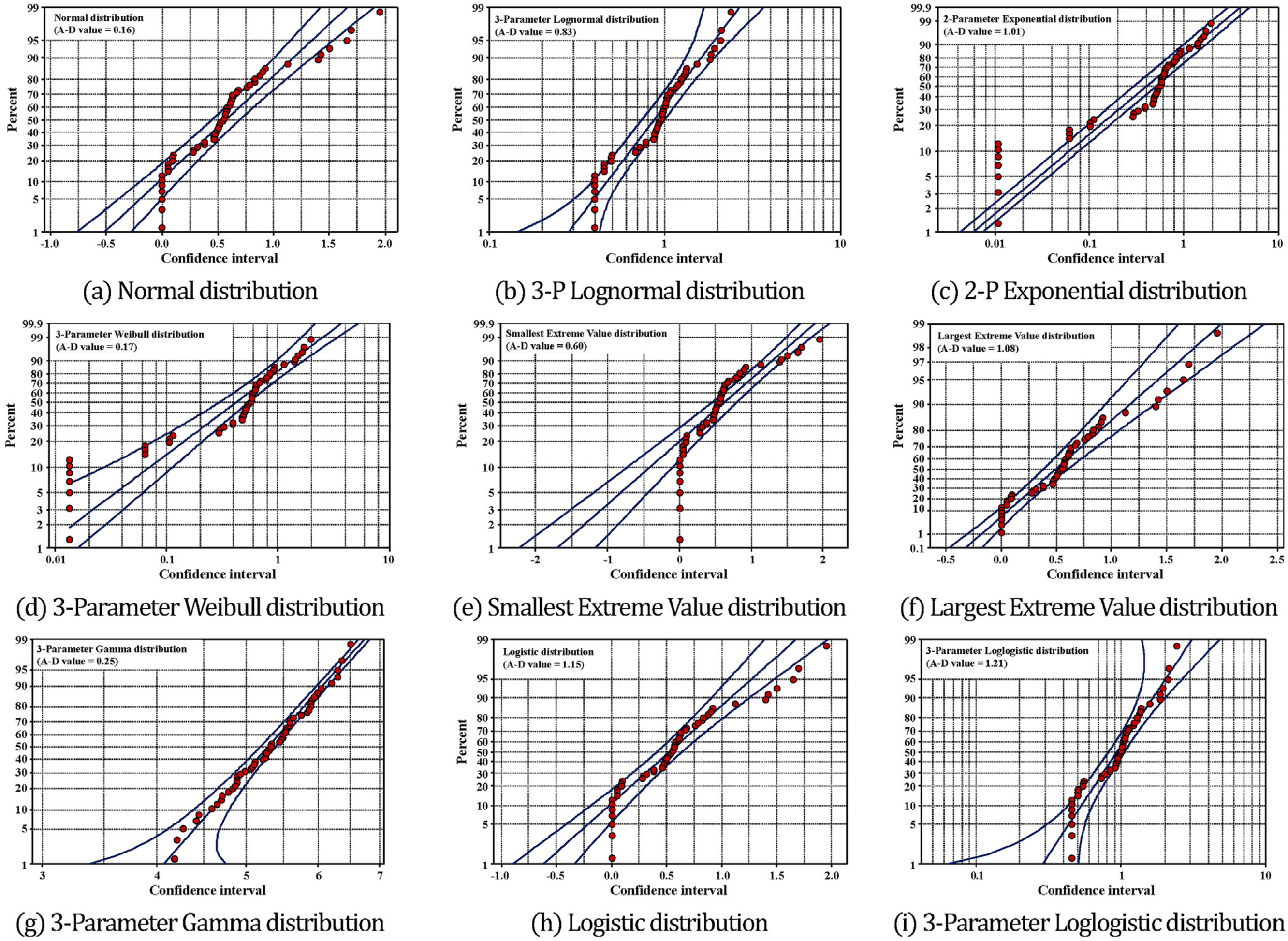

Fig. 4. Example results on goodness of fit test results from Anderson-Darling test.

Table 2
Example of the goodness of fit test (by Anderson-Darling test method).

Probability density functions	Time data set					Average
	Data 1	Data 2	Data 3	Data 4	Data 5	
Normal	**0.16**	1.67	2.06	2.14	1.87	1.58
3-Parameter Lognormal	0.17	1.35	1.05	**0.83**	12.66	3.21
2-Parameter Exponential	5.67	2.64	1.45	1.01	2.37	2.63
3-Parameter Weibull	0.17	2.50	1.54	1.14	2.97	1.66
Smallest Extreme Value	0.60	3.57	4.43	4.19	3.48	3.25
Largest Extreme Value	0.67	1.18	1.16	0.98	**1.08**	**1.01**
3-Parameter Gamma	0.25	3.25	2.21	1.82	8.78	3.26
Logistic	0.23	**1.15**	1.27	1.47	1.44	1.11
3-Parameter Loglogistic	0.23	1.21	**0.89**	1.08	3.64	1.41

3.2.6. *Formulation of sub-parameter of probability density function as a function of time (Step 6)*

The formulation of sub-parameters of selected best-fit PDFs as a function of time can then be conducted by utilising the obtained "overall outcome" from the previous step (Key step II). From the example shown in Table 2, the largest extreme value distribution was selected as the overall outcome. Hence, it should be reminded that the selected best-fit PDF is shown in Eq. (1), which represents the typical case by Table 2. By the end of this paper, a generalised corrosion model will be proposed considering all cases as shown in Tables A1 and A2.

Selected best-fit distribution (Example)

$$\textit{probability density } (PD) = f(x) = \left(\frac{1}{B}\right) \cdot \exp\left[-\frac{(x-A)}{B}\right] \cdot \exp\left[-\exp\left\{-\frac{(x-A)}{B}\right\}\right] \tag{1}$$

where, PD = probability density, x = horizontal axis which represents "corrosion depth ($=D_c$)" in the present study, A = shape parameter, and B = scale parameter.

In Eq. (1), there are two (2) sub-parameters of the largest extreme value distribution such as shape and scale parameters. The selected sub-parameters can then be plotted versus time as shown in Fig. 5. For the formulation of sub-parameters as a function of time, the empirical formulation can be obtained based on the plotted data using the curve-fitting method. In this case, two (2) empirical formulations were obtained for shape and scale parameters. This may be considered the most important part of this stage and empirical formulations should well fit the original data.

From the obtained empirical formulation of sub-parameters by time presented in Fig. 5, the optimised outcome can be obtained. Basically, the main difference between overall and optimised outcome is the values of sub-parameters, which is clearly presented in Fig. 5. This means that the two outcomes are achieved based on selected best-fit PDF, where the largest extreme value distribution was selected in the previous example, and the only difference is the sub-parameter value. As shown in Fig. 5, the overall outcome is based on plotted dots, while optimised outcome is achieved based on obtained empirical formulation presented by a dotted line as a function of time. The example of optimised outcome can be observed in Fig. A1(c).

The following Eq. (2) represents the typical type of optimised outcome by adopting the largest extreme value distribution.

$$PDF = f(D_c) = \left(\frac{1}{B(t_e)}\right) \cdot \exp\left[-\frac{(D_c - A(t_e))}{B(t_e)}\right] \cdot \exp\left[-\exp\left\{-\frac{(D_c - A(t_e))}{B(t_e)}\right\}\right] \quad (2)$$

where, D_c = corrosion depth, $A(t_e)$ = shape parameter as a function of exposure time, $B(t_e)$ = scale parameter as a function of exposure time, and t_e = exposure time.

In the next step, the formulation of corrosion model considering time will be focused to provide a user-friendly solution.

3.2.7. Formulation of time-dependent corrosion wastage models (Step 7)

In this study, two types of time-dependent corrosion wastage models such as 1) mean and standard deviation-based model and 2) cumulative density function-based model, are introduced. These

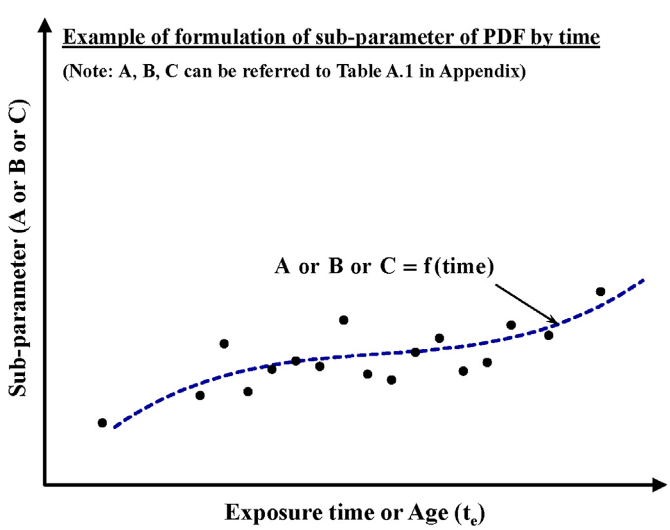

Fig. 5. Schematic view for the formulation of sub-parameter of probability density function by time (Paik and Kim, 2012).

- Optimised outcome (Key step III)

two obtained corrosion models will be harmonised to propose the final outcome in Step 8.

- Model I: Mean and Standard Deviation based model (Step 7a)

Once the optimised outcome is obtained, mean and standard deviation can then be obtained as shown in Table A2. The mean and standard deviation of the largest extreme value distribution, selected as the best-fit PDF shown in Eq. (2) by the previous example in Table 2, are illustrated in Eqs. (3.1) and (3.2), respectively. Thus, it should be highlighted that the obtained mean and standard deviation are the functions of time, while sub-parameters, i.e., shape (A) and scale (B) are presented as $A(t_e)$ and $B(t_e)$.

$$M = A(t_e) + 0.5772B(t_e) \quad (3.1)$$

$$SD = \sqrt{(\pi^2 B(t_e)^2)/6} \quad (3.2)$$

where, M = Mean, and SD = Standard deviation.

With regards to model I, the following five (5) levels of corrosion models in Eq. (4) are proposed in the present study to classify the degree of corrosion. In general, the mean or 95% and above band data, based on corrosion depth information illustrated in Fig. 6(a), is used for the development of corrosion model. Previously, Paik and Thayamballi (2003) defined three corrosion model types such as 1) convex, 2) linear, and 3) concave as shown in Fig. 6(b). In the present study, the method to propose more refined time-dependent corrosion wastage model than the existing model shown in Fig. 6(b) is introduced.

In the case of abovementioned "largest extreme value" distribution case, harmonisation process (Step 8) with Model II (Step 7b) can then be skipped, because the mean (M) and standard deviation (SD) values can directly be obtained from Eqs. (3.1) and (3.2). Therefore, harmonisation can be defined as the determination of the coefficient of Model II based on the comparison between Model I and Model II results. Details can be referred to in Step 8, shown in Section 3.2.8.

Proposed Corrosion Model (Model I)

$$D_c = \begin{cases} M - SD & \text{for Slight level} \\ M & \text{for Average level} \\ M + SD & \text{for Severe level I} \\ M + 2SD & \text{for Severe level II} \\ M + 3SD & \text{for Severe level III} \end{cases} \quad (4)$$

where, D_c = Corrosion depth ($\neq$ negative value), M = Mean, and SD = Standard deviation.

If M and SD values are hard to be obtained using simple calculations, then Model II needs to be further developed. For example, the calculation of Gamma function "Γ", which is included in the Weibull, 3-parameter Weibull, Log-logistic, 3-parameter log-logistic, etc., in Table A2, may not be obtained easily by hand calculation. This means that additional processing (Model II) is required to provide a simplified corrosion model, which will be introduced in Step 7b. Lastly, the readers can also use other types of PDFs, which will provide different mean and standard deviation equations as shown in Table A2.

- Model II: Cumulative density function based model (Step 7b)

The cumulative density function (CDF) concept is applied to propose corrosion model II. In the case of the largest extreme value distribution being selected as the best-fit PDF, M and SD can easily be obtained as presented in Eqs. (3.1) and (3.2). This means that

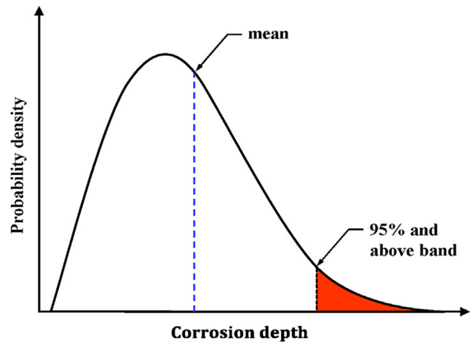

(a) Definition of mean and 95% and above band

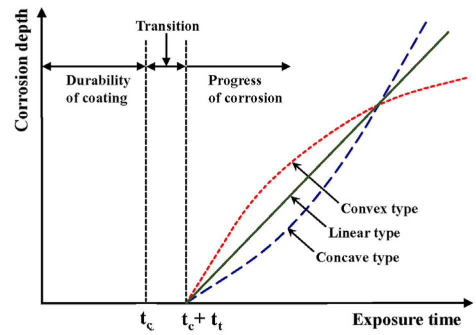

(b) Existing corrosion model types

Fig. 6. Example of existing corrosion models (Paik and Thayamballi, 2003, 2007).

additional process in terms of the development of Model II, and harmonisation step can be skipped. However, the detailed procedure to propose Model II for the selected best-fit distribution, which contains simplified M and SD, is documented for the better understanding of the readers. In this case, the obtained Model II should produce exactly the same results as Model I after conducting the harmonisation step. The following Eq. (5) shows a typical example of CDF representing the largest extreme value distribution that was derived using integration of PDF from Eq. (2). In addition, the features of PDF and CDF are well presented in Fig. 7.

$$CDF = F\left(D_c\right) = 1 - \exp\left[-\exp\left(\frac{D_c - A(t_e)}{B(t_e)}\right)\right] \tag{5}$$

where, CDF = cumulative density function, $A(t_e)$ = shape parameter as a function of exposure time, $B(t_e)$ = scale parameter as a function of exposure time, and t_e = exposure time (or year).

Once CDF is obtained by integration of PDF, the 2nd corrosion model (herein Model II) is then rearranged based on corrosion depth (D_c) as shown in Eq. (6) from Eq. (5).

Proposed Corrosion Model (Model II)

$$D_c = A(t_e) + B(t_e) \cdot \ln[-\ln(1 - CDF)] \tag{6}$$

Based on the obtained corrosion model II, the discussions on how the CDF value illustrated in Eq. (6) will be covered in the Harmonisation step (Step 8).

3.2.8. Harmonisation of the corrosion models (Step 8)

- Harmonised outcome (Key step IV)

In this step, the proposed model I and II are compared to decide the value of CDF in Eq. (6) which means that Model I and II are assumed to be equal as follows.

$$Model\ I \simeq Model\ II \tag{7}$$

Therefore, five (5) values of CDFs for different corrosion levels such as slight level, average level, and severe level I, II, and III, can be obtained from Eq. (7) as shown in Fig. 8 and Fig. A1(d). The details of this harmonisation step may be referred in the application part covered in Part II. Some cases of corrosion data input, there might be difficult to generate CDF due to the mathematical issue. As shown above, Model I and Model II may produce reasonably similar outcomes. Therefore, one model that could be obtained is thought to be sufficient if there is issue on conversion from PDF to CDF.

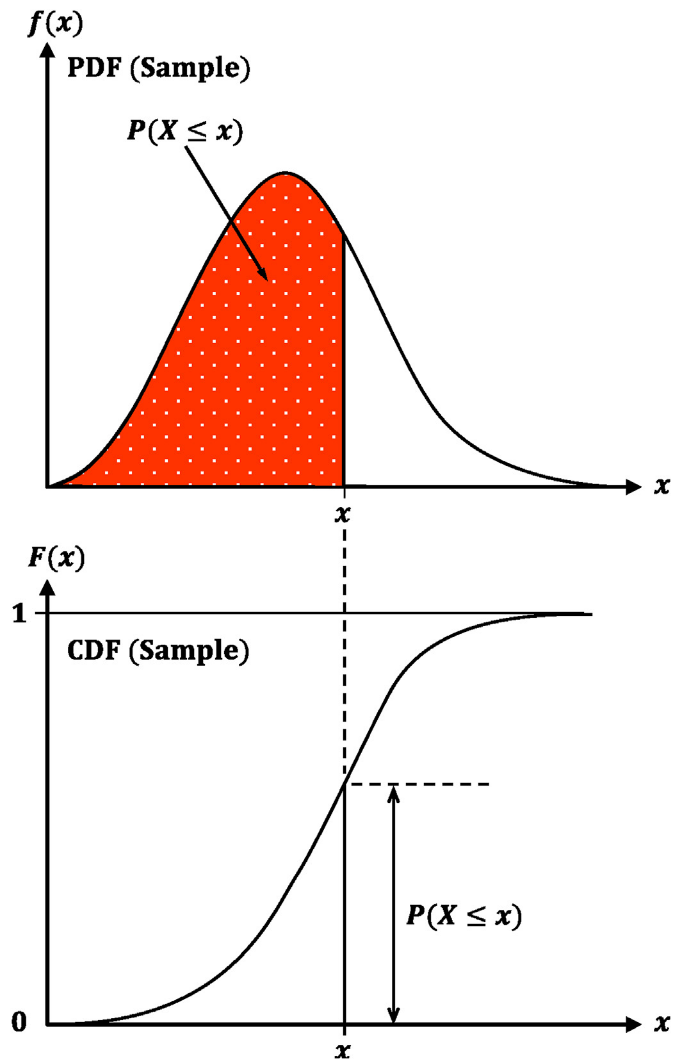

Fig. 7. Features of probability density (PDF) and cumulative density functions (CDF).

3.2.9. Generalisation of time-dependent corrosion model by mathematical formulation (Step 9)

From the previous Step 8, harmonisation between Model I and II was conducted and verified using the coefficient of determination (R^2) value. If the R^2 value is above 0.9, it can then go through the generalisation step for the mathematical formulation of time-dependent corrosion model. If the R^2 value does not satisfy criterion ($R^2 = 0.9$), it can then go back to Step 5 where the 2nd best PDF can be selected as the best-fit PDF.

In this last step, simplified mathematical formulations, which represent the time-dependent corrosion wastage in five levels as illustrated in Eq. (4), are proposed. From the obtained outcome, engineers can easily predict the corrosion by time and this may help to make relevant plans for repairs or estimation of decommissioning of the corroded structures. In addition, the starting of the corrosion time can also be backtracked from the obtained simplified corrosion formulation; if the corrosion depth is set as zero (0) then the time can be calculated and it can be assumed as the starting of corrosion time.

4. Concluding remarks

Nowadays, numerous ships and offshore structures are approaching the end of their life cycle. Corrosion is one of the issues in aging structures as it degrades the structures. The accuracy of deterministic assessment method, which is the current practice in the industry, is questionable due to the inherent uncertainties that govern the result of the assessment. The use of linear corrosion growth model for estimating the corrosion is too conservative for the current oil and gas industry that are experiencing oil price downturn. To provide cost-effective safety assessment of structure, this study aimed to develop an advanced technique to obtain time-dependent corrosion wastage model of metal structure for assessing the corrosion progression of the aging structure. Based on developed technique, simplified software was developed as shown in Appendix B. The proposed technique in Part I is also verified by ship's ballast water corrosion data in Part II. Lastly, the limitation of proposed method in this study should be clearly stated so that it could be supplemented through further research. If the measured corrosion wastage information (input data) does not show a constant tendency, it is difficult to obtain a smooth fitting curve illustrated in Fig. 5. This might produce unsuitable results to use in the corrosion model developed. In addition, the best way to collect corrosion data might be using real time sensor systems. If it is impossible, it should be measured at least at three different time zones, and the more measurements the higher the results can be obtained.

The proposed method's procedure is briefly summarised as follows:

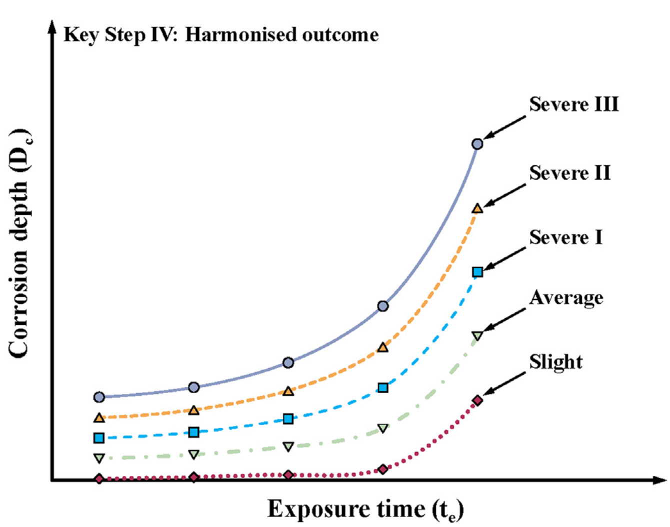

Fig. 8. Example of obtained harmonised outcomes.

- The proposed method adopted a probabilistic approach to determine the distribution of corrosion depth for each year.
- A generalised method to propose nonlinear corrosion model by time is introduced in detail using the best-fit probability density function.
- Corrosion depth is formulated as a function of years using mean, standard deviation, and cumulative distribution calculation approach.

The strengths of the proposed method are also briefly summarised as follows:

- A less conservative but accurate way to estimate the nonlinear corrosion depth of the structure by time is proposed.
- Starting time of corrosion can be predicted.
- The remaining life of a structure can be predicted by adopting the obtained time-dependent corrosion wastage model and it will be very useful for the planning of maintenance and repairing.
- This approach provides an option for the industry to operate structures as close to their maximum capacity while ensuring the safety of the structure.

Acknowledgements

This research was supported by the Technology Innovation Program (Grant No.: 10053121 and 10051279) funded by the Ministry of Trade, Industry & Energy (MI, Korea). The authors would also like to thank Newcastle University for their financial supports.

Appendix. Supplementary data

Supplementary data to this article can be found online at https://doi.org/10.1016/j.ijnaoe.2020.06.007.

References

Abdussamie, N., Ojeda, R., Daboos, M., 2018. ANFIS method for ultimate strength prediction of unstiffened plates with pitting corrosion. Ships Offshore Struct. 13 (5), 540–550.

Akpa Jackson, G., 2013. Modeling of the corrosion rate of stainless steel in marine oil environment. ARPN J. Eng. Appl. Sci. 8 (8), 656–662.

Bai, Y., Yan, H.B., Cao, Y., Kim, Y.H., Yang, Y.Y., Jiang, H., 2016. Time-dependent reliability assessment of offshore jacket platforms. Ships Offshore Struct. 11 (6), 591–602.

Cheng, A., Chen, N.Z., 2017. Corrosion fatigue crack growth modelling for subsea pipeline steels. Ocean Eng. 142, 10–19.

Chernov, B.B., 1990. Predicting the corrosion of steels in seawater from its physiochemical characteristics. Protect. Met. 26 (2), 238–241.

Chernov, B.B., Ponomarenko, S.A., 1991. Physiochemical modelling of metal corrosion in seawater. Protect. Met. 27 (5), 612–615.

Commercial, Specialised Diving LTD, 2018. Are Your Underwater Structures in a Good Condition? – UT Meter, Commercial Blog. Ferndown, UK. https://commercialandspecialiseddiving.wordpress.com/2018/02/28/are-your-underwater-structures-in-a-good-condition-ut-meter/.

Cui, J., Wang, D., Ma, N., 2019. Case studies on the probabilistic characteristics of ultimate strength of stiffened panels with uniform and non-uniform localized corrosion subjected to uniaxial and biaxial thrust. Int. J. Naval Archit. Ocean Eng. 11 (1), 97–118.

Energy Global News, 2020. 12 December 1999 – Tanker Erika Broken in Two in the Bay of Biscaye. Energy Global News. http://www.energyglobalnews.com/12-december-1999-tanker-erika-broke-in-two-in-the-bay-of-biscaye.

Evans, U.R., 1960. The Corrosion and Oxidation of Metals: Scientific Principles and Practical Applications. Edward Arnold Publishers Ltd., London, UK.

Georgiadis, D., Samuelides, M., 2019. A methodology for the reassessment of hull-girder ultimate strength of a VLCC tanker based on corrosion model updating. Ships Offshore Struct. 14 (Suppl. 1), 270–280.

Gucuyen, E., Erdem, R.T., 2014. Corrosion effects on structural behaviour of jacket type offshore structures. Gradevinar 66 (11), 981–986.

Guedes Soares, C., Garbatov, Y., Zayed, A., Wang, G., 2005. Non-linear corrosion model for immersed steel plates accounting for environmental factors. Transactions of the SNAME 111, 194–211.
Ivanov, L.D., Chen, N.Z., 2017. On the presentation of ship's hull girder section modulus in probabilistic formats. Ships Offshore Struct. 12 (8), 1024–1036.
Ivošević, Š., Meštrović, R., Kovač, N., 2019. Probabilistic estimates of corrosion rate of fuel tank structures of aging bulk carriers. Int. J. Naval Archit. Ocean Eng. 11 (1), 165–177.
Joo, M., Doh, J.H., Lee, J.S., 2018. Determination of the best distribution and effective interval using statistical characterization of uncertain variables. J. Comput. Design Eng. 5 (3), 358–367.
Kim, D.K., Kim, S.J., Kim, H.B., Zhang, X.M., Li, C.G., Paik, J.K., 2015. Ultimate strength performance of bulk carriers with various corrosion additions. Ships Offshore Struct. 10 (1), 59–78.
Kim, D.K., Kim, B.J., Seo, J.K., Kim, H.B., Zhang, X.M., Paik, J.K., 2014a. Time-dependent corrosion damage on the development of residual strength – grounding damage index diagram. Ocean Eng. 76, 163–171.
Kim, D.K., Kim, H.B., Zhang, X.M., Li, C.G., Paik, J.K., 2014b. Ultimate strength performance of tankers associated with industry corrosion addition practices. Int. J. Naval Archit. Ocean Eng. 6 (3), 507–528.
Kim, D.K., Park, D.K., Kim, H.B., Seo, J.K., Paik, J.K., Kim, B.J., Kim, M.S., 2012a. The necessity of applying the common corrosion addition rule to container ships in terms of ultimate longitudinal strength. Ocean Eng. 49, 43–55.
Kim, D.K., Park, D.K., Kim, J.H., Kim, S.J., Kim, B.J., Seo, J.K., Paik, J.K., 2012b. Effect of corrosion on the ultimate strength of double hull oil tankers - Part I: stiffened panels. Struct. Eng. Mech. 42 (4), 507–530.
Kim, D.K., Park, D.K., Park, D.H., Kim, H.B., Kim, B.J., Seo, J.K., Paik, J.K., 2012c. Effect of corrosion on the ultimate strength of double hull oil tankers - Part II: hull girders. Struct. Eng. Mech. 42 (4), 531–549.
Kim, D.K., Zalaya, M.A., Choi, H.S., Mohd Hairil, M., Park, K.S., 2017. Safety assessment of corroded jacket platform considering decommissioning event. Int. J. Automot. Mech. Eng. 14 (3), 4462–4485.
Kim, D.K., Lim, H.L., Cho, N.K., 2020. An advanced technique to predict time-dependent corrosion damage of onshore, offshore, nearshore and ship structures: Part II = application to the ship's ballast tank. Int. J. Naval Archit. Ocean Eng. https://doi.org/10.1016/j.ijnaoe.2020.07.002. In press.
Kim, D.K., Lim, H.L., Yu, S.Y., 2019a. Ultimate strength prediction of T-bar stiffened panel under longitudinal compression by data processing: a refined empirical formulation. Ocean Eng. 192, 106522.
Kim, D.K., Wong, E.W.C., Lee, E.B., Yu, S.Y., Kim, Y.T., 2019b. A method for empirical formulation of current profile. Ships Offshore Struct. 14 (2), 176–192.
Lam, C., 2015. Statistical Analyses of Historical Pipeline Incident Data with Application to the Risk Assessment of Onshore Natural Gas Transmission Pipelines. MSc Dissertation, The University of Western Ontario, London, Canada.
Mohd Hairil, M., Kim, D.K., Kim, D.W., Paik, J.K., 2014a. A time-variant corrosion wastage model for subsea gas pipelines. Ships Offshore Struct. 9 (2), 161–176.
Mohd Hairil, M., Paik, J.K., 2013. Investigation of the corrosion progress characteristics of offshore subsea oil well tubes. Corrosion Sci. 67, 130–141.
Mohd Hairil, M., Kim, D.W., Lee, B.J., Kim, D.K., Seo, J.K., Paik, J.K., 2014b. On the burst strength capacity of an aging subsea gas pipeline. J. Offshore Mech. Arctic Eng. 136 (4), 041402, 1-7.
Melchers, R.E., 2003a. Mathematical modelling of the diffusion controlled phase in marine immersion corrosion of mild steel. Corrosion Sci. 45 (5), 923–940.
Melchers, R.E., 2003b. Modeling of marine immersion corrosion for mild and low alloy steels – Part 1: phenomenological model. Corrosion 59 (4), 319–334.
Melchers, R.E., 2003c. Probabilistic model for marine corrosion of steel for structural reliability assessment. J. Struct. Eng. 129 (11), 1484–1493.
Melchers, R.E., 2008. Development of new applied models for steel corrosion in marine applications including shipping. Ships Offshore Struct. 3 (2), 135–144.
Meo, D.D., Oterkus, E., 2017. Finite element implementation of a peridynamic pitting corrosion damage model. Ocean Eng. 135, 76–83.
Paik, J.K., Kim, D.K., 2012. Advanced method for the development of an empirical model to predict time-dependent corrosion wastage. Corrosion Sci. 63, 51–58.
Paik, J.K., Kim, S.K., Lee, S.K., 1998. Probabilistic corrosion rate estimation model for longitudinal strength members of bulk carriers. Ocean Eng. 25 (10), 837–860.
Paik, J.K., Lee, J.M., Hwang, J.S., Park, Y.I., 2003a. A time-dependent corrosion wastage model for the structures of single- and double-hull tankers and FSOs and FPSOs. Mar. Technol. 40 (3), 201–217.
Paik, J.K., Melchers, R.E., 2008. Condition Assessment of Aged Structures. CRC Press, New York, USA.
Paik, J.K., Thayamballi, A.K., 2003. Ultimate Limit State Design of Steel-Plated Structures. John Wiley & Sons, Chichester, UK.
Paik, J.K., Thayamballi, A.K., 2007. Ship-shaped Offshore Installations. Cambridge University Press, Cambridge, UK.
Paik, J.K., Thayamballi, A.K., Park, Y.I., Hwang, J.S., 2003b. A time-dependent corrosion wastage model for bulk carrier structures. Int. J. Marit. Eng. 145 (A2), 61–87.
Paik, J.K., Thayamballi, A.K., Park, Y.I., Hwang, J.S., 2004. A time-dependent corrosion wastage model for seawater ballast tank structures of ships. Corrosion Sci. 46 (2), 471–486.
Qin, S., Cui, W., 2003. Effect of corrosion models on the time-dependent reliability of steel plated structures. Mar. Struct. 16 (1), 15–34.
Rahbar-Ranji, A., Niamir, N., Zarookian, A., 2015. Ultimate strength of stiffened plates with pitting corrosion. Int. J. Naval Archit. Ocean Eng. 7 (3), 509–525.
Rajput, A., Park, J.H., Noh, S.H., Paik, J.K., 2019. Fresh and sea water immersion corrosion testing on marine structural steel at low temperature. Ships Offshore Struct. in-press https://www.tandfonline.com/doi/full/10.1080/17445302.2019.1664128.
Ringsberg, J.W., Li, Z., Johnson, E., Kuznecovs, A., Shafieisabet, R., 2018. Reduction in ultimate strength capacity of corroded ships involved in collision accidents. Ships Offshore Struct. 13 (Suppl. 1), 155–166.
Tomashov, N.D., 1966. Theory of Corrosion and Protection of Metals: the Science of Corrosion. Macmillan, New York, USA.
Wang, G., Lee, A.K., Ivanov, L., Lynch, T.J., Serratella, C., Basu, R., 2008. A statistical investigation of time-variant hull girder strength of aging ships and coating life. Mar. Struct. 21 (2–3), 240–256.
Wikipedia, 2018. Goodness of Fit. https://en.wikipedia.org/wiki/Goodness_of_fit.
Wong, E.W.C., Kim, D.K., 2018. A simplified method to predict fatigue damage of TTR subjected to short-term VIV using artificial neural network. Adv. Eng. Software 126, 100–109.
Wood, M.H., Vetere Arellano, A.L., Van Wijk, L., 2013. Corrosion-related Accidents in Petroleum Refineries: Lessons Learned from Accidents in EU and OECD Countries (Report No. EUR 26331 EN). European Commission Joint Research Centre, Institute for the Protection and Security of the Citizen, Ispra, Italy.
Yang, H.Q., Zhang, Q., Tu, S.S., Wang, Y., Huang, Y., 2016. A study on time-variant corrosion model for immersed steel plate elements considering the effect of mechanical stress. Ocean Eng. 125, 134–146.
Zhang, Y., Huang, Y., Zhang, Q., Liu, G., 2016. Ultimate strength of hull structural plate with pitting corrosion damnification under combined loading. Ocean Eng. 116, 273–285.